# PROCEEDINGS OF SPIE

SPIEDigitalLibrary.org/conference-proceedings-of-spie

Monitoring of tissue heating with medium intensity focused ultrasound via four dimensional optoacoustic tomography

Francisco Javier Oyaga Landa, Silvia Ronda Penacoba, Xosé Luís Deán-Ben, Francisco Montero de Espinosa, Daniel Razansky

Francisco Javier Oyaga Landa, Silvia Ronda Penacoba, Xosé Luís Deán-Ben, Francisco Montero de Espinosa, Daniel Razansky, "Monitoring of tissue heating with medium intensity focused ultrasound via four dimensional optoacoustic tomography," Proc. SPIE 10494, Photons Plus Ultrasound: Imaging and Sensing 2018, 104945J (19 February 2018); doi: 10.1117/12.2288939



Event: SPIE BiOS, 2018, San Francisco, California, United States

# Monitoring of tissue heating with medium intensity focused ultrasound via four dimensional optoacoustic tomography

Francisco Javier Oyaga Landa,  $^{1,2}$  Silvia Ronda Penacoba,  $^3$  Xosé Luís Deán-Ben,  $^1$  Francisco Montero de Espinosa,  $^3$  and Daniel Razansky  $^{1,2,*}$ 

<sup>1</sup>Institute for Biological and Medical Imaging (IBMI), Helmholtz Zentrum München, Neuherberg, Germany

<sup>2</sup>School of Medicine, Technische Universität München (TUM), Munich, Germany <sup>3</sup>ITEFI-CSIC, Institute of Physics and Communication Technologies, Madrid, Spain \*Corresponding author: dr@tum.de

#### ABSTRACT

Medium intensity focused ultrasound (MIFU) holds promise in important clinical applications. Generally, the aim in MIFU is to stimulate physiological mechanisms that reinforce healing responses, avoiding reaching temperatures that can cause permanent tissue damage. The outcome of interventions is then strongly affected by the temperature distribution in the treated region, and accurate monitoring represents a significant clinical need. In this work, we showcase the capacities of 4D optoacoustic imaging to monitor tissue heating during MIFU. The proposed method allows localizing the ultrasound focus, estimating the peak temperature and measuring the size of the heat-affected volume. Calibration experiments in a tissue-mimicking phantom demonstrate that the optoacoustically-estimated temperature accurately matches thermocouple readings. The good performance of the suggested approach in real tissues is further showcased in experiments with bovine muscle samples.

**Keywords:** Photoacoustic Imaging; Thermal Imaging; Temperature; Ultrasound diagnostics.

# 1. INTRODUCTION

Ultrasound therapy consists of a series of techniques commonly used in clinics for treatments ranging from kidney stones to injured muscles and tendons.<sup>1</sup> The majority of ultrasound(US) treatments include a subproduct of thermal effects produced via tissue heating with average intensity levels exceeding those permitted for diagnostic US imaging purposes. The use of high-intensity focused ultrasound (HIFU) is to selectively destroy abnormal tissues, such as malignant neoplastic lesions, via local temperature elevations exceeding the coagulation thresholds.<sup>2</sup> HIFU has been also used at power levels below the thresholds required for ablation, such as in intense therapy ultrasound (ITU), e.g. by creating thermal injury zones in the tissue, initiating tissue repair cascade, promoting collagen generation and thus a healing response.<sup>4,5</sup> Low intensity pulsed ultrasound (LIPUS) has also shown beneficious effects in tissue healing.<sup>3</sup> In addition, non-thermal physical effects, such as cavitation and acoustic streaming, have shown to influence cell membrane permeability and increase cellular activity.<sup>6</sup> Medium intensity focused ultrasound (MIFU), with acoustic intensity levels between those used in echography and HIFU, represents a largely unexplored scientific niche that can lead to combined and cooperative thermal and non-thermal physical effects in soft tissues for performing physical or cancer therapy, either directly or via local drug delivery. Dedicated and flexible electronics with programmable parameters voltage, signal shape, frequency and number of active elements as well as specialized US array transducers need to be studied and developed to elucidate existing uncertainties in US physiotherapy. Specifically, heating results from the absorption of US waves in the tissue, while other effects, such as cavitation or acoustic streaming, may additionally take place. Efficacy of US treatments calls for precise monitoring of the spatio-temporal temperature map during the intervention, control over the delivered US intensity degree and time span of the treatment.<sup>7</sup>

It is well known that several inconsistencies in the clinical results for different ultrasound therapy protocols have been reported.<sup>8</sup> The development of an efficient monitoring method is thus necessary for the improvement of the therapeutic outcome while dodging unwanted tissue destruction. Of particular importance is the feasibility to render real-time feedback on the spatio-temporal temperature distribution in the treated tissue. Heat-driven cell deterioration typically starts at temperatures above 50°C, while cell death strongly depends on the exposure

Photons Plus Ultrasound: Imaging and Sensing 2018, edited by Alexander A. Oraevsky, Lihong V. Wang, Proc. of SPIE Vol. 10494, 104945J ⋅ © 2018 SPIE ⋅ CCC code: 1605-7422/18/\$18 ⋅ doi: 10.1117/12.2288939

duration to a certain temperature.<sup>3</sup> For instance, cell death can take up to several minutes to occur at 50°C, while equivalent damage is produced within seconds for temperatures above 60°C.<sup>9</sup> Temperature monitoring is also essential in MIFU for controlling the exposure time at lower temperatures and preventing overheating. Intrusive temperature monitoring methods based on thermocouples, thermistors or fiber-optic detectors can be used for temperature control.<sup>10</sup> However, those are invasive approaches that can only retrieve temperature readings from a limited number of discrete locations. Volumetric mapping of temperature fields was further investigated using non-invasive imaging techniques.<sup>11</sup> Nonetheless, previous non-invasive approaches lack enough penetration depth, contrast, spatial or temporal resolution for real-time volumetric temperature mapping.

In this work, we propose optoacoustic (OA) imaging as an advantageous approach for monitoring clinical thermal interventions as it has shown to provide high sensitivity to changes in temperature and can further detect variations in tissue optical properties due to coagulation levels.<sup>12,13</sup> To this end, OA monitoring and guidance has been used to control thermal therapies involving radio-frequency ablation, <sup>14</sup> laser-induced thermotherapy, <sup>15</sup> cryoablation, therapeutic US procedures including HIFU or nanoparticle-based targeted therapies. <sup>16</sup> One of the best assets of the OA method is the possibility to integrate it with MIFU or HIFU using the same transducer array. <sup>17</sup> Yet, real-time volumetric mapping of the temperature distribution during US thermotherapy, particularly for intensity levels below the thermal damage thresholds, has never been attempted. Here, we use a novel MIFU electronic custom-made system and a three-dimensional piezoelectric spherical-shaped matrix array. We further showcase the feasibility of 4D optoacoustic coagulation monitoring and mapping of temperature distribution in ex-vivo bovine tissue during MIFU heating.

#### 2. MATERIALS AND METHODS

The lay-out of the experimental set-up is depicted in Figure 1a. MIFU heating was induced with a self-made annular array built with 8 equiareal coaxial rings, enabling the focus of the US beam along the axial direction at an arbitrary point. Each single element of the array has an area of  $0.88 \ cm^2$  and a central working frequency of 2 MHz. The array has a total diameter of 3 cm. The elements were excited with a custom-made multichannel electronic driving system (Sitau, Dasel, Spain) regulated through a MATLAB script. The excitation signals in each element were delayed in order to focus the US beam by constructive interference within a  $0.04 \ cm^3$  volume located at a distance of 5 cm from the active surface. When driven with a negative square pulse of 150 V, peak pressure of 3 MPa is generated at the focus, which corresponds to  $300 \ W/cm^2$  of acoustic intensity.<sup>4</sup> The pressure was measured with a needle hydrophone (DAPCO 54389) with  $0.6 \ mm$  active diameter.

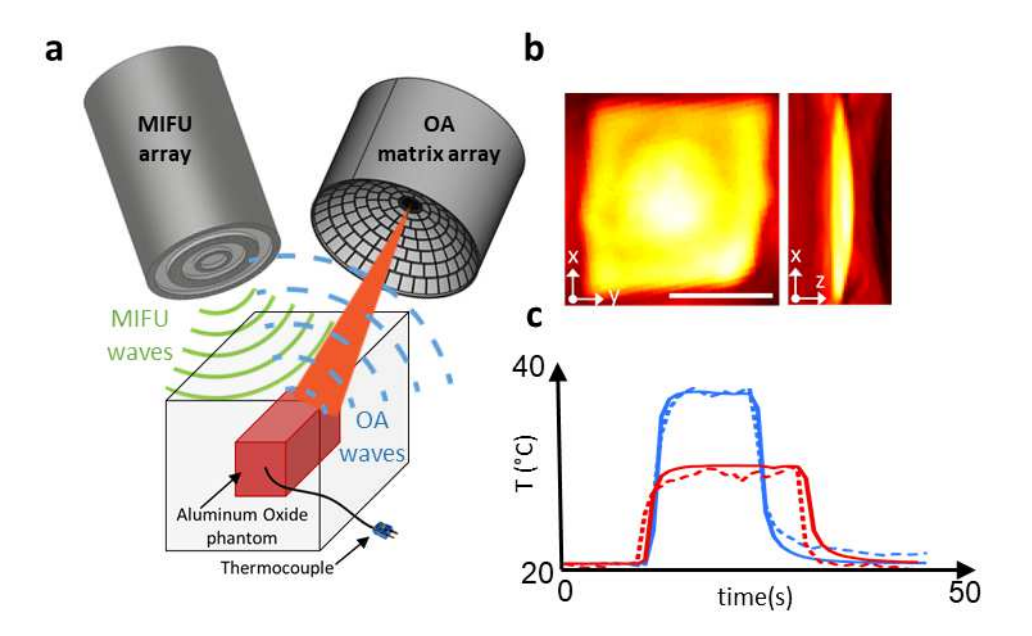


Figure 1. Schematic view of the experimental setup. (a) Drawings of the transducer array and the US system. (b) Transverse MIP optoacoustic images of the front and side views of the phantom. (c) Optoacoustic temperature estimations (dashed lines) using the approach proposed in the Method section. The thermocouple readings (continuous lines) from the same color, represent the two different US heating procedures, at 255 (blue) and 125 (red) cycles.

Real-time OA volumetric temperature monitoring was achieved with a customized spherical matrix array composed of 256 piezoelectric elements with  $90^{\circ}$  (0.59 $\pi$  solid angle) angular coverage. Each element of the array has an area of  $3x3 \ mm^2$ , central frequency of 4 MHz and >80% detection bandwidth, providing a nearly isotropic imaging resolution of 200  $\mu$ m around the geometrical center of the sphere. <sup>18</sup> The OA detection array was positioned orthogonally with respect to the MIFU array and acoustic coupling was guaranteed by immersing the entire set-up in water (Figure 1a). Optoacoustic responses were excited with a short-pulsed (<10 ns) tunable laser source (Innolas Laser GmbH, Krailling, Germany) guided via a custom-made fiber bundle (CeramOptec GmbH, Bonn, Germany) through a cylindrical cavity in the center of the array. Optical fluence of  $11 \text{ mJ}/cm^2$ was measured at the surface of the sample at an illumination wavelength of 720 nm. The pulse repetition frequency of the laser source was set to 10 Hz. The 256 optoacoustic signals were simultaneously acquired at 40 mega-samples per second (MSPS) by a custom-made data acquisition (DAQ) system (Falkenstein Mikrosysteme GmbH, Taufkirchen, Germany) triggered with the Q-switch output of the laser. Synchronization between OA imaging and MIFU excitation was achieved by delaying the US excitation tone-bursts by 100  $\mu$ s with respect to the laser trigger used for the OA signal acquisition. Specifically, the employed MIFU excitation protocol consisted of emitting 50 tone-bursts of 125 or 255 cycles with 150 V negative square amplitude and carrier frequency of 2 MHz, at a pulse repetition frequency (PRF) of 1 KHz following each laser pulse. OA images were reconstructed with a graphics processing unit (GPU)-based three-dimensional back-projection algorithm. <sup>19</sup> Preceding the reconstruction, the OA raw signals were first acquired and then deconvolved with the known impulse response of the array elements and filtered with band-pass frequencies between 0.1 MHz and 6 MHz.

### 2.1 Temperature Estimation Method

The proposed OA temperature estimation approach is based on the nature of the optoacoutic signals and their dependence on temperature. Stress confinement can be assumed when the optoacoustic response are excited with a short-duration pulsed laser.<sup>20</sup> Under these conditions, the initial OA pressure wave is given by  $p_0 = \Gamma \mu_a \phi$ , being  $\Gamma$  the (dimensionless) Grüneisen parameter,  $\mu_a$  the optical absorption coefficient and  $\phi$  the light fluence. The

temperature dependance of the generated OA signals mainly comes from variations in the Grüneisen parameter. In the water-like aqueous media, these variations can be given by  $^{20}$ 

$$\Gamma(T) = 0.0043 + 0.0053T \tag{1}$$

being T expressed in °C. The relative change of the OA signal as a function of the temperature increase  $\Delta T$  can be then expressed as where T is expressed in °C. Note that Equation 1 has been previously verified with empirical measurements across a wide range of temperatures.<sup>21</sup> According to Equation 1, the relative change of the OA signal as a function of temperature increase  $\Delta T$  can be then expressed as<sup>22</sup>

$$\frac{\Delta p_0}{p_{0,0}} = \frac{0.0053\Delta T}{0.0043 + 0.0053 \cdot T_0} \tag{2}$$

being  $p_{0,0}$  and  $T_0$  the baseline OA signal and the initial temperature, respectively, before the application of MIFU heating.  $\Delta p_0$  is the increase in OA signal with respect to  $p_{0,0}$ . According to Equation 2, the amplitude of the OA signals is expected to increase by approximately 2.7% per degree for temperature levels around 36°C in living biological tissues. The temperature increment can then be estimated from the relative OA signal increase as

$$\Delta T = \frac{\Delta p_0(0.8113 + T_0)}{p_{0.0}} \tag{3}$$

# 2.2 Phantom validation experiments

First, an 8.5 mm side square-shaped tissue-mimicking phantom was analytically tested to showcase the validity of Equation 3. The phantom consisted of a 1.3% w/w agar powder solved in water matrix, mixed with 7.8% w/w of Aluminum Oxide  $(Al_2O_3)$  and India ink to create an US absorption coefficient of 3.6 dB $cm^{-1}$  at 2 MHz frequency and an optical absorption coefficient of  $\mu_a$  3.5  $cm^{-1}$  at an illumination wavelength of 720 nm. A thermocouple (Physitemp Instruments Inc., Clifton, New Jersey) was inserted at the front (illuminated) edge of the phantom. The temperature readings were digitized with an integrated NI 9213 DAQ (National Instruments Corporation, Austin, Texas, U.S.). The OA-based temperature estimation approach, described in Equations 1-3, was used to estimate the temperature at a region of interest (ROI) corresponding to the known location of the thermocouple. In the same way, the US focus was pointed to the tip of the thermocouple by inducing the maximum temperature elevation at the sensor location.

#### 2.3 Ex-vivo bovine tissue experiments

The effectiveness of the proposed approach for temperature mapping in real tissues was subsequently examined in an ex-vivo bovine sample. In a first step, the capability to localize the US focus in a three-dimensional region was tested. For this, the MIFU array was scanned along the axial direction of the OA imaging probe. For each position, the MIFU array was driven as previously described. Considering that no significant thermal diffusion occurs within this time period, the temperature raise for each burst is assumed to be solely due to US absorption. In addition, the spatio-temporal distribution of temperature was estimated during MIFU heating for a fixed position of the US focus. The baseline tissue temperature was  $T_0 = 22^{\circ}$ C. MIFU heating was stopped after 20 s while the OA monitoring continued for additional 40 s to cover the cooling period.

#### 3. RESULTS

Figure 1a shows a schematic representation of the measurement arrangement. The maximum intensity projection (MIP) along the transversal and sagittal direction of the volumetric OA images taken before the MIFU heating is displayed in Figure 1b. The temperature increase in the phantom at the thermocouple location was then estimated following Equation 3. Specifically, two measurements were performed. In the first one, a series of 150 V tone-bursts consisting of 255 cycles were used to excite the MIFU array for 25 s. The temperature values as a function of time measured with the thermocouple and estimated from the OA image sequence are respectively displayed by the continuous and dashed blue lines in Figure 1c respectively. In a second measurement, a series of tone-bursts of 150 V and 125 cycles were used to drive the MIFU array for 30 s. The relative OA signal increases

were estimated with a reference OA image (the baseline signal) taken as the average of 30 frames immediately preceding the MIFU procedure.

The discrepancies can be attributed to the approximate nature of Equation 3,<sup>23</sup> which was derived by assuming that the variations in the Grüneisen parameter of the phantom are equivalent to those in water. Additional inaccuracies may originate from the discrepancy between the actual location of the thermocouple tip and the analyzed OA traces.

# 3.1 Temperature mapping in ex-vivo bovine tissue

The results of the temperature mapping experiment in an ex-vivo bovine tissue sample are shown in Figure 2. Specifically, the spatio-temporal maps of the temperature elevation estimated according to Equation 3 are displayed in Figure 2a. It can be seen that the temperature map estimated for the time point of peak temperature elevation (Figure 2a, 17 s) is tightly centered around the ultrasonic focus location.

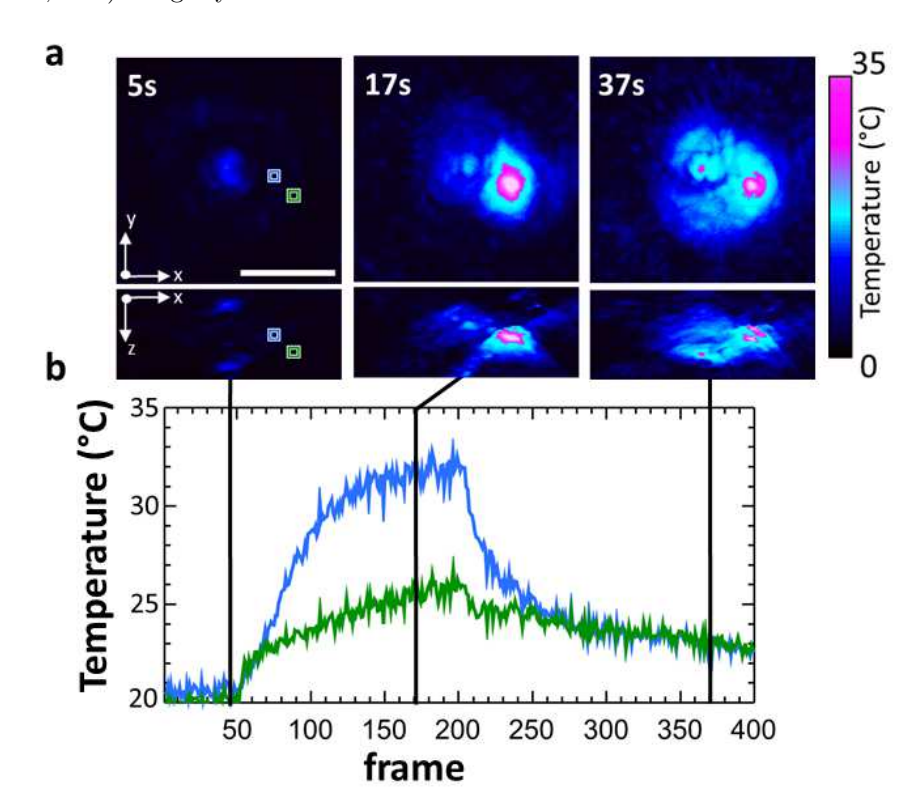


Figure 2. Volumetric optoacoustic monitoring of temperature during MIFU therapy performed in an ex-vivo bovine tissue (Scale bar = 5mm). (a) Transverse and lateral MIPs of the reconstructed optoacoustic volumes at different time points along the procedure. (b) Time corresponding to the different treatment phases, being 5s before the MIFU system was switched on, 17s at the maximum heating stage and 37s at the post-treatment thermal expansion period.

On the other hand, the heated region spreads over a larger region at later time points during the cooling period (Figure 2a, 37 s), which indicates that thermal diffusion plays a dominant role in carrying the heat further away from the ultrasonic focus. This is further corroborated in the time traces in Figure 2b, corresponding to the estimated temperatures at two locations indicated in Figure 2a at 5 s.

# 4. DISCUSSION AND CONCLUSION

Therapeutics using medium intensity focused ultrasound intents to establish advancements in adequacy, reliability, safety and traceability of US treatments in both drug delivery and physiotherapy. In this work, 4D OA

tomography was used to non-invasively compute the temperature increase in tissues by a novel designed MIFU prototype scheme. Of particular importance is the feasibility to provide real-time volumetric temperature feedback, which can greatly impact the outcome of MIFU-based medical treatments by 1) enabling effective control of the exposure time of the target tissue at a given temperature and 2) preventing tissue overheating above the damage threshold. OA is particularly suitable for temperature mapping applications due to the high sensitivity of the Grüneisen parameter, representing the OA conversion efficiency, to temperature variations.  $^{24}$  Note that in our current experiments the temperature distribution was estimated by assuming the Grüneisen parameter to be equivalent to that of water, although it can be further calibrated and adjusted to the treated tissue. The high spatio-temporal resolution of the state-of-the art OA tomography system employed further represents an important advantage. In this work, we have attained spatial resolution of 200  $\mu$ m at 10 Hz volumetric frame rates, which covers well the spatio-temporal range of the induces temperature variations. Higher spatial and temporal resolutions are also possible by using a similar configuration, which however would come to the detriment of the field of view.  $^{23}$ 

Four-dimensional OA tomography further enables dynamic localization of the position of the US focus. In this way, more accurate identification of the target tissues can be facilitated prior to applying the therapy. Naturally, the SNR of the differential OA images declines with depth due to light attenuation, the latter dominating over acoustic attenuation for the applicable US frequency range. <sup>16</sup> In order to improve on the achievable monitoring depth, other light delivery methods, e.g. based on endoscopic or intravascular probes, may be additionally considered. <sup>24</sup> Registration of OA and US images can further provide enhanced anatomical information and some efficient techniques for hybrid optoacoustic-ultrasound (OPUS) imaging have been recently reported. <sup>25, 26</sup>

The monitoring approach introduced in this work can also be potentially applied in treatments based on selective tissue destruction with HIFU. These procedures can particularly benefit from augmented information acquired by means of multispectral optoacoustic tomography (MSOT) analysis.<sup>16</sup> The most recently developed OA systems effectively provide five-dimensional (real-time three-dimensional multispectral) imaging capabilities, thus enabling tracking of spectroscopic variations in the target tissue, e.g. due to coagulation.<sup>27</sup> It should be noted that the temperature dependence of the OA signals in biological tissues is significantly altered at temperatures exceeding 50°C,<sup>28</sup> so that more accurate calibration are needed for temperature monitoring in coagulated tissue volumes. At the same time, optical attenuation in biological tissues has to be taken into account when deriving temperature with the proposed methodology, so that within a region of interest, the higher temperature increment and OA contrast will benefit the accuracy of the estimate. Development of proper models accounting for thermal effects occurring in living organisms at temperatures beyond the coagulation thresholds thus represent an important next step.

In conclusion, we demonstrate a new high resolution volumetric temperature monitoring method during US heating based on real-time acquisition of three-dimensional optoacoustic data. The achieved high sensitivity to temperature variations, high spatial resolution and fast imaging rates anticipate applicability of the suggested approach in various procedures involving low and medium intensity therapeutic US, such as physical rehabilitation, <sup>1,8</sup> pain management or neurostimulation. The method suggested is expected to improve the safety and efficacy of US treatments and to advance the general applicability of US-based therapy.

#### ACKNOWLEDGMENTS

The authors acknowledge support from the German Research Foundation (DFG) under Research Grant RA 1848/5-1 (D.R.) and the Spanish Ministry of Economy and Competitiveness under project DPI2016-80254-R (F.M.).

# REFERENCES

- 1. ter Haar, G. European Journal of Ultrasound. 9, 3–9, (1999).
- 2. Kim, Y., Rhim, H., Choi, M.J., Lim, H.K. & Choi, D. Korean J. Radiol. 9(4), p. 291–302, (2008).
- 3. Chu, K.F. & Dupuy, D.E. Nature Reviews Cancer. 14, p. 199–208, (2014).
- Mast, T.D., Makin, I.R., Faidi, W., Runk, M.M., Barthe, P.G. & Slayton, M.H. J. Acoust. Soc. Am. 118, p. 2715–24, (2005).
- 5. Slayton, M.H. & Barton, J.K. IEEE International Ultrasonic Symposium., 1654–1657, (2014).

- 6. Dyson, M. Br. J. of Cancer 5, p. 165–171, (1982).
- Fuhrmann, T.A., Georg, O., Haller, J., Jenderka, K. & Wilkens, V. Journal of Therapeutic Ultrasound. 4(28), (2016).
- 8. Robertson, V.J. & Baker, K.G. Phys. Ther. 81(7), p. 1339–50, (2001).
- 9. Haemmerich, D. Crit. Rev. Biomed. Eng. 38, p. 53–63, (2010).
- 10. Saccomandi, P., Schena, E. & Silvestri, S. International Journal of Hyperthermia. 29, p. 609-619, (2013).
- 11. Lewis, M.A., Staruch, R.M. & Chopra, R. International Journal of Hyperthermia. 31, p. 163–181, (2015).
- 12. Petrova, E.V. et. al. *Optics Express.* **21**(21), p. 25077–90, (2013).
- 13. Gao, L. et. al. Journal of Biomedical Optics 18(2), 026003, (2013).
- 14. Pang, G.A., Bay, E., Deán-Ben, X.L. & Razansky, D. *Journal of cardiovascular electrophysiology.* **26**(3), p. 339–345, (2015).
- 15. Oyaga Landa, F. J. et. al. Optics letters. 41, p. 2704–2707, (2016).
- 16. Deán-Ben, X.L. et. al. Chemical Society Reviews. 46(8), p. 2158–2198, (2017).
- 17. Prost, E. et. al. J. Biomedical Opt. 17(6), 061205, (2012).
- 18. Deán-Ben, X.L. & Razansky, D. Optics Express. 21, 28062–71, (2013).
- 19. Deán-Ben, X.L., Ozbek, A. & Razansky, D. IEEE transactions on medical imaging. 32(11), 2050–55, (2013).
- 20. Wang, L.V. & Wu, H. Biomedical optics: principles and imaging. John Wiley & Sons. (2012).
- 21. Wang, W. & Mandelis, A. Biomedical Optics Express. 5, p. 2785–90, (2014).
- 22. Oyaga Landa, F.J., Deán-Ben, X.L., Sroka, R. & Razansky, D. Scientific Reports. 7(1), 9695, (2017).
- 23. Deán-Ben, X.L. et. al. Light: Science & Applications. 5, e16201, (2016).
- 24. Hailong, H., Buehler, A. & Ntziachristos, V. SPIE Proc. 9708, (2016).
- 25. Fehm, T.F., Deán-Ben, X.L. & Razansky, D. SPIE Proc. 9323, (2015).
- 26. Pajek, D. & Hynynen, K. Phys. Med. Biol. 57(15), p. 4951-68, (2012).
- 27. Deán-Ben, X.L. & Razansky, D. Light: Science and Applications. 3(1), e137, (2014).
- 28. Oyaga Landa, F. J., Deán-Ben, X.L. & Razansky, D. SPIE Proc. 10064, (2017).